Geophysical Research Letters

RESEARCH LETTER
10.1029/2018GL079421

Ionization of the Polar Atmosphere by Energetic Electron Precipitation Retrieved From Balloon Measurements

I. A. Mironova[1], A. A. Artamonov[2], G. A. Bazilevskaya[3], E. V. Rozanov[4,5], G. A. Kovaltsov[6], V. S. Makhmutov[3], A. L. Mishev[7,8], and A. V. Karagodin[1]

[1]Faculty of Physics, Department of Physics of Earth, St. Petersburg State University, St. Petersburg, Russia, [2]Research Institute for Space Medicine, Federal Research Clinical Center of Federal Biomedical Agency of Russia, Moscow, Russia, [3]Lebedev Physical Institute, Russian Academy of Science, Moscow, Russia, [4]PMOD/WRC and IAC ETHZ, Davos Dorf, Switzerland, [5]Western Department of Pushkov Institute of Terrestrial Magnetism, Ionosphere and Radio Waves Propagation, Russian Academy of Sciences, Kaliningrad, Russia, [6]Ioffe Physical-Technical Institute, St. Petersburg, Russia, [7]Space Climate Research Unit, University of Oulu, Finland, [8]Sodankylä Geophysical Observatory, Oulu, Finland

Key Points:
- Ionization rates (IR) from energetic electron precipitation (EEP) are calculated using balloon observations and compared to the CMIP6 data set
- The difference in the atmospheric response calculated with these two data sets can exceed 100% for NO_x and reach 25% for O_3
- IR obtained from balloon measurements reveal a high temporal variability, which is absent in CMIP6 data

Correspondence to:
I. A. Mironova,
i.a.mironova@spbu.ru

Citation:
Mironova, I. A., Artamonov, A. A., Bazilevskaya, G., Rozanov, E., Kovaltsov, G. A., Makhmutov, V. S., et al. (2019). Ionization of the polar atmosphere by energetic electron precipitation retrieved from balloon measurements. *Geophysical Research Letters*, *46*, 990–996. https://doi.org/10.1029/2018GL079421

Received 2 JUL 2018
Accepted 21 DEC 2018
Accepted article online 27 DEC 2018
Published online 16 JAN 2019

Abstract

We retrieve ionization rates in the atmosphere caused by energetic electron precipitation from balloon observations in the polar atmosphere and compare them against ionization rates recommended for the Phase 6 of the Coupled Model Intercomparison Project. In our retrieval procedure, we consider the precipitating electrons with energies from about tens of keV to 5 MeV. Our simulations with 1-D radiative-convective model with interactive neutral and ion chemistry show that the difference of the Phase 6 of the Coupled Model Intercomparison Project and balloon-based ionization rate can lead to underestimation of the NO_x enhancement by more than 100% and ozone loss up to 25% in the mesosphere. The atmospheric response is different below 50 km due to considering highly energetic electrons, but it is not important because the absolute values of atmospheric impact is tiny. Ionization rates obtained from the balloon observations reveal a high variability.

Plain Language Summary

The main idea of our manuscript is to demonstrate that the atmospheric ionization rates (IR) can be successfully retrieved from the long-term balloon observations of the energetic electron precipitation (EEP) events and used to evaluate the uncertainties of the other IR data sets, for example, IR recommended for the Phase 6 of the Coupled Model Intercomparison Project (CMIP6). IR obtained from the balloon observations reveal a high variability. This means that the time resolution used in CMIP6 probably is not enough to consider high frequency variability of the precipitating electron fluxes. Using 1-D radiative-convective model with neutral and ion chemistry, we compared the atmospheric response to the one particular EEP observed by balloons and presented in CMIP6 data. We show that the difference of the CMIP6 and balloon-based IRs can lead to underestimation of the NO_x enhancement by more than 100% and ozone loss by up to 25% in the mesosphere. Our results are new and needed for the understanding of the potential uncertainties in CMIP6 EEP forcing. Our paper will give inspiration for the continuation of the balloon measurements of EEP-related processes using improved instruments.

1. Introduction

Several recent papers (Andersson et al., 2014; Arsenovic et al., 2016; Meraner & Schmidt, 2017; Rozanov et al., 2012; Seppälä et al., 2015; Smith-Johnsen et al., 2018; Turunen et al., 2016) have led to growing interest from the science community to the influence of energetic electrons on atmospheric chemistry and climate. For the first time, both components of the solar forcing (i.e., spectral solar irradiance and energetic particle precipitation) were included in the forcing set recommended for the climate models participating in the Coupled Model Intercomparison Project (Phase 6; Eyring et al., 2016; Matthes et al., 2017). Atmospheric effects of solar protons and cosmic rays are well recognized (Calisto et al., 2011; Funke et al., 2011; Jackman et al., 2008; Mironova et al., 2015). However, the extent to which energetic electron precipitation (EEP) have an influence upon polar atmospheric chemistry, including the ozone layer, and climate is not yet fully characterized and understood (e.g., Andersson et al., 2014; Matthes et al., 2017). EEP from the outer radiation belt can have energies ranging from tens of keV up to several MeV. The electrons with these energies are known as middle range energy electrons (MEE). MEE mainly ionize the polar atmosphere above 60 km in the subauroral zone (Arsenovic et al., 2016; van de Kamp et al., 2016), with an ionization maximum at about 80–90-km altitude (Mironova et al., 2015) or 70–100 km (van de Kamp et al., 2018) for the EEP energy ranges 30–300 keV. Some papers have suggested that high EEP with energies from 100 keV up to several MeV can produce ionization in the atmosphere down to 20 km and even deeper (Artamonov et al., 2016a, 2017; Makhmutov et al., 2016). Information about EEP is usually obtained by satellite instruments, such as National Oceanic and Atmospheric Administration Polar-orbiting Operational Environmental Satellites (e.g., Nesse Tyssøy et al., 2016) or Van Allen Probes (e.g., Shprits et al., 2016). Some information can also be obtained from observation of radio wave propagation (Clilverd et al., 2017). Precipitating energetic electrons also generate X-ray and gamma-ray bremsstrahlung which can be detected by stratospheric balloon experiments (Makhmutov et al., 2016; Millan et al., 2013; Woodger et al., 2015). These measurements can provide additional insights into the properties of EEP.

The calculated daily mean MEE ionization rates (IR) for the period from preindustrial time to present day were recommended for the use by the climate model groups participating in CMIP6 project (Matthes et al., 2017). However, an independent evaluation of the provided data has not been performed yet. These daily mean IR are based on the empirical model reconstruction of the EEP spectra of the precipitating electrons from the daily A_p or *Dst* indices (van de Kamp et al., 2016). EEP is a result of a complicated sequence of processes, including solar-wind-magnetosphere coupling; acceleration of electrons up to several MeV from the seed population provided by the solar wind through various mechanisms acting on different time scales; and scattering of electrons which leads to violation of adiabatic invariants. A variety of these processes leads to strong variability of EEP and their dependence on the interplanetary disturbance type, site of observation, local magnetic time, and energy of precipitating electrons. A high EEP interdaily variability has been observed in many experiments (Clilverd et al., 2017; Cresswell-Moorcock et al., 2013; Mironova et al., 2015; Nesse Tyssøy et al., 2016; Woodger et al., 2015). Moreover, the electron energy spectrum used for the IR calculations in the CMIP6 project (Matthes et al., 2017) was limited (to 30 keV to <1 MeV), and the lack of electrons with higher energies can lead to some underestimation of the IR below 1 hPa (altitude less than ~50 km). Thus, evaluation of the CMIP6 IR accuracy is necessary to understand potential problems in the models driven by this forcing.

In this paper, we present IR induced by EEP based on the balloon observations of ~500 EEP events (Makhmutov et al., 2016). For the calculation of the IR, we use an approach based on the energy spectrum obtained from the balloon observations and include the contribution of precipitating electrons with energies above 1 MeV. We compare our results with the daily mean IR recommended for CMIP6 (Matthes et al., 2017) and estimate the implications of the obtained differences for atmospheric chemistry. Our results allow independent evaluation of this data set, which is important for its potential future users.

2. Variability of EEP-Induced Ionization in the Polar Atmosphere

To calculate IR in the atmosphere during the EEP, we used the spectra of precipitated electrons obtained from balloon observations of secondary cosmic rays in the atmosphere performed in the Murmansk region (geomagnetic latitude about 64°N). This long-lasting experiment has run from 1957 up to now (Stozhkov et al., 2009). The balloon launches were performed every day, or more often, in 1957–1990 and three times a week since 1991. The energy of precipitating electrons can be estimated from the depth of penetration of the bremsstrahlung X-ray radiation into the atmosphere. Approximately 55% of the EEP events detected in the atmosphere with energies E between ~ 200 and 1,300 keV. EEP with $E < 200$ keV was observed in ~9% of events and EEP with $E > 1{,}300$ keV in 36% of events. Bremsstrahlung X-ray generated by precipitating electrons with energy above ~300 keV is recorded in this experiment at altitudes 20–35 km (Makhmutov et al., 2016). An energy spectrum of precipitating electrons at the top of the atmosphere presented in Makhmutov et al. (2016) was retrieved from X-ray absorption using simulations of the electron transport through the atmosphere (Makhmutov et al., 2003). The electron spectrum was fitted with an exponential law: $F_e(E) = A_e * exp(-E/E_0)$, where $F_e(E)$ is differential isotropic flux ($keV^{-1} \cdot cm^{-2} \cdot s^{-1}$) of precipitating electrons with energy E, E_0 (keV) is the characteristic energy parameter. In the paper of Comess et al. (2013) and Millan and Thorne (2007), the spectral fitting with an exponential law has also been used such spectral-type. Incoming fluxes of precipitating electrons are subject of rapid fluctuations; therefore, the spectra retrieved from balloon observations are averaged over time of observations. The time interval for which the X-rays can be observed is usually shorter than 30 min, during which "an EEP snapshot" with 1-min

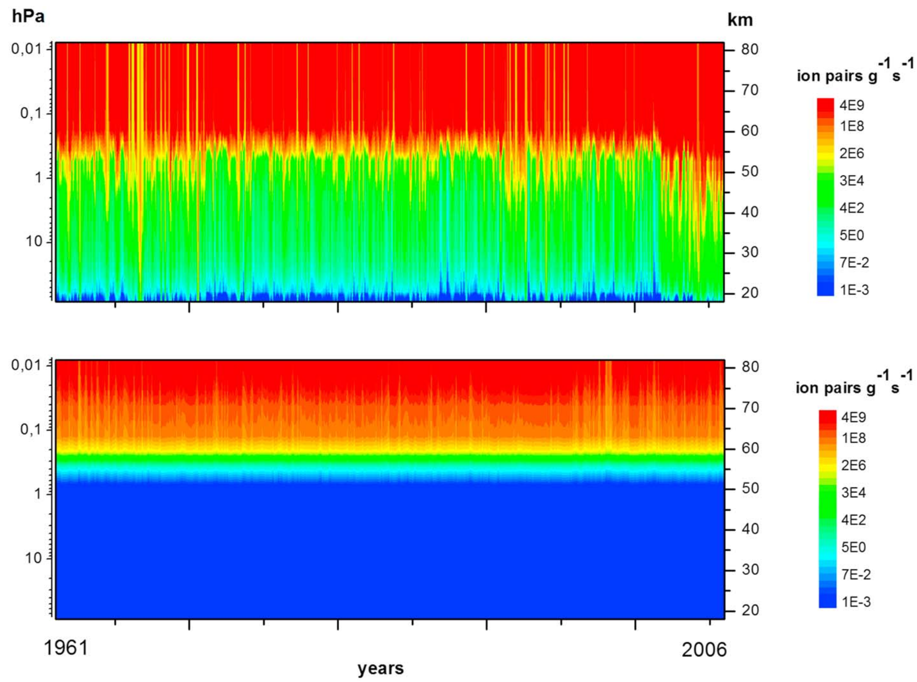

Figure 1. Ionization of the atmosphere during energetic electron precipitation. (top) IR are calculated for energetic electron precipitation in 1961–2006 observed with balloons. IR are depicted for the days from the Makhmutov et al. (2016) catalog. (bottom) Daily IR from Coupled Model Intercomparison Project Phase 6 data set for the same days. IR = ionization rates.

resolution is recorded. The time of EEP observations was 08–14 UT (around 10–17 Magnetic Local Time). About 500 intensive EEP events were recorded in 1961–2014 and compiled in the catalog by Makhmutov et al. (2016; http://sites.lebedev.ru/ru/DNS_FIAN/479.html).

For our IR computations, we use the ionization yield function for mono-energetic electrons (Artamonov et al., 2016a) obtained from the simulations of electron transport through the Earth atmosphere performed with PLANETOCOSMICS code and atmospheric composition from NRLMSISE-00 model (Picone et al., 2002). The modification of this yield function for isotropic precipitating electrons has been presented by Artamonov et al. (2017). The parametrization of ionization (Artamonov et al., 2016a, 2017) takes into account bremsstrahlung effect in the atmosphere down to 100 hPa. The yield function allows to calculate vertical IR profiles, if the energy spectrum and flux are known from either observations or models.

Figure 1 presents the time series of atmospheric ionization, showing the variability of atmospheric ionization during EEP events for selected days of the 20th to 23rd solar cycles. We calculated IR profiles for 487 days during 1961–2006 from EEP spectra catalog (Makhmutov et al., 2016). The results of our calculation are presented on the top panel of Figure 1. We note that Figure 1 is not a continuous time history of EEP observations because IR are shown on the event-by-event basis, skipping days where no events were observed, and which are not presented in the (Makhmutov et al., 2016) catalog.

The bottom panel of Figure 1 illustrates variations of atmospheric ionization by EEP events taken from the CMIP6 data set (Matthes et al., 2017; http://solarisheppa.geomar.de/cmip6) at the geomagnetic latitude 63.75°N and for the same days as shown on the top panel of Figure 1. The CMIP6 IR were determined using both the EEP parametrization of van de Kamp et al. (2016) based on A_p and *Dst* indices and the ionization yield functions of Fang et al. (2010) with atmospheric composition from NRLMSISE-00 model of Picone et al. (2002). The ionization yield functions of Fang et al. (2010) can only be applied to precipitating electrons with energies $E < 1$ MeV and does not work below about 1 hPa.

CMIP6 electron IR are for medium-energy electrons only. They explicitly exclude the auroral electrons, as the purpose was to provide MEE for high-top climate models which already include auroral electrons. The EEP forcing of CMIP6 also excludes the highly relativistic electrons of energies of more than 1 MeV.

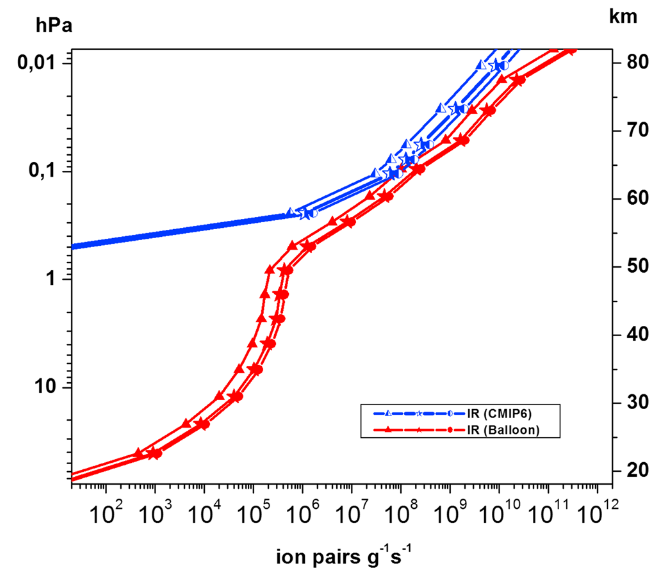

Figure 2. Statistical features of IR variability derived from the balloon measurements (red lines) and CMIP6 data (blue lines) during 1961–2006. Median IR profiles = lines with stars. 75% IR profiles = lines with circles. 25% IR profiles = lines with triangles. IR = ionization rates; CMIP6 = Coupled Model Intercomparison Project Phase 6.

At about 0.01 hPa (~80 km) level, the IR on the top and bottom panels of Figure 1 look similar rather, but they deviate substantially at lower altitudes. At higher pressures, the IR from balloon observations demonstrate gradual decrease toward the tropopause, while the ionization from CMIP6 data practically disappears below 0.5 hPa (altitude less than ~55 km). Differences in the IR altitude profiles in CMIP6 data and calculations using balloon measurements are related to the effects of electrons with energies above 1 MeV that produce corresponding gamma-ray and X-ray bremsstrahlung. Some part of these differences can be explained by the different spectrum parametrizations applied by Makhmutov et al. (2016; an exponential fit) and van de Kamp et al. (2016; power law). The IR cutoff below about 1 hPa in the CMIP6 data is due to the cutoff of MEE energy spectra at 1 MeV.

The IR depicted on the top panel of Figure 1 demonstrate much higher temporal variability, even between 0.1 and 1 hPa (between 50 and 65 km) levels, than IR on the bottom panel, although IR are shown for the same days on both panels. However, one should keep in mind that IR from balloon observations relate to a single geographical location and short time interval, while van de Kamp et al. (2016) IR represent zonal and daily mean values.

Figure 2 shows some statistical characteristics of IR profiles illustrated in Figure 1. IR profiles shown in red demonstrate IR obtained by balloon measurements, while CMIP6 IR profiles are shown in blue. Figure 2 demonstrates that median profiles in both data sets (blue and red lines with stars) are close to each other in 65–80-km altitude band with difference by about less than 10 times. A noticeable difference appears at lower altitudes and can reach several orders of magnitude.

Below the 1 hPa layer (altitude less than ~50 km), the IR profiles obtained from balloon measurements demonstrate IR and variability on a daily scale due to bremsstrahlung initiated by high energy electrons. Ionization for these altitudes is virtually absent in CMIP6 data because electrons with higher than 1-MeV energy and gamma-ray and X-ray emissions are not considered.

The IR derived from the balloon observation demonstrates a large variability reflected by a wide corridor between the minimum and maximum IR values. It is caused by large variability that is an intrinsic feature of the electron precipitation which was not accounted for EEP forcing in CMIP6.

The systematic underestimation of CMIP6 IR can be also a result of using only one Medium Energy Proton and Electron Detector telescope for obtaining MEE spectra (van de Kamp et al., 2016).

3. Atmospheric Response to EEP-Induced Ionization

Variability of ionization during energetic particles precipitation can lead to significant changes in the polar neutral atmosphere through the formation of odd nitrogen (NO_x) and odd hydrogen (HO_x), followed by ozone depletion. These effects will be more noticeable in the polar winter atmosphere where the solar UV is virtually absent. In our study, we estimate the response of the charged and neutral components of atmosphere to various EEP events using the 1-D radiative-convective model with interactive neutral and ion chemistry (Shapiro et al., 2011). The model is covering the atmosphere from ground up to about 90 km and treats radiation, neutral and ion chemistry, convective adjustment, and vertical diffusion processes. The model is transient and driven by time-varying external conditions such as solar irradiance and IR. At every 1-hr time step, the model calculates heating/cooling rates in solar and infrared spectral regions and changes of the temperature as well as the concentration of 43 neutral and 57 charged components. The convective adjustment activates if the temperature gradient in the troposphere exceeds predefined climatological value. We apply the model for a single geographical location over Murmansk (68°N) where the balloon measurements took place. We carry out 1-year long model run without any EEP starting from first day of the year. This run can be used as reference to estimate the influence of EEP during any particular period. The timing for the one specific atmospheric impact simulations was determined as local early winter, and the ionization

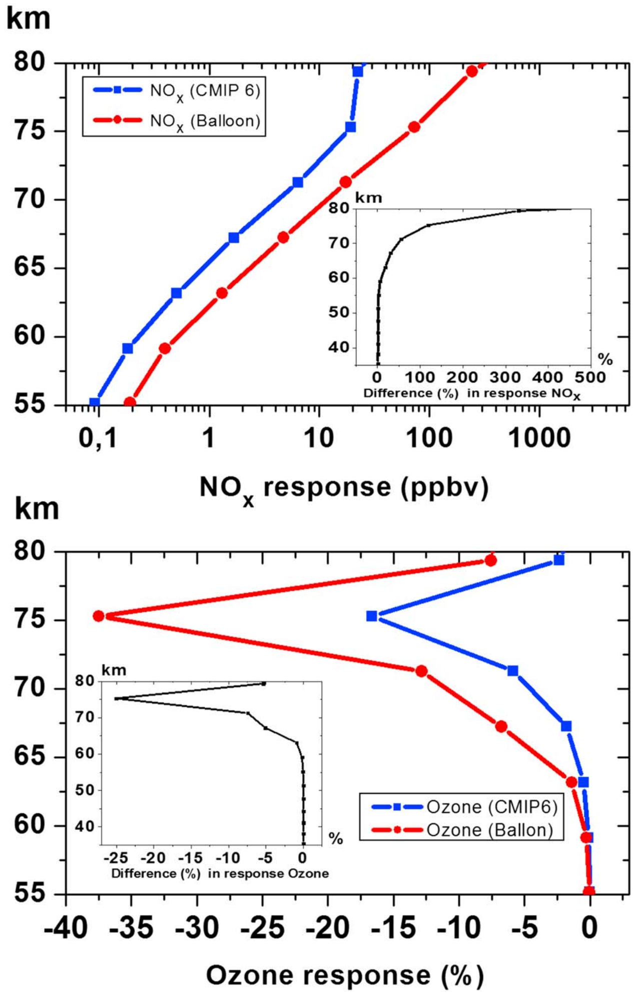

Figure 3. Response of NO_x (top, ppbv) and ozone (bottom, %) to energetic electron precipitation simulated with ionization rates from balloon measurements (red line) and CMIP6 data (blue line). Black line shows difference (%) in absolute values of NO_x and zone mixing ratio as respond according to CMIP6 and balloon data sets. The results are shown for the noon at the day after the event. CMIP6 = Coupled Model Intercomparison Project Phase 6.

event was introduced on the 331st day of the year. We carry out two additional 1-year long model runs starting from first day of the year. The two experiment runs were driven by IR from either CMIP6 data or balloon observations. Therefore, the influence of EEP on the atmospheric chemistry is represented by the difference of the chemical fields between experiments and reference run. The comparison of CMIP6 with the balloon data is not straightforward because we should compare the influence of the zonal and daily mean CMIP6 IR against balloon measurements for particular location and time. However, they are perfectly comparable, because it is how CMIP6 IR supposed to be implemented for climate model. For example, the climate model over the Murmansk at 10 UT should use zonal and daily mean CMIP6. Therefore, we can compare CMIP6 with balloon data for these time and location and illustrate the difference.

For the investigation, we selected the median IR profiles of EEP forcing of CMIP6 (blue lines with stars, see Figure 2) and calculated from balloon measurements of EEP flux (red line with stars, see Figure 2). These median IR profiles differ by about 10 times at 55–80-km layer.

The NO_x and ozone responses to the median IR shown in Figure 2 are presented in Figure 3. The results are shown for the noon of the day after the event. For the calculations of the atmospheric state with 1-D model, it was assumed that the applied IR are daily mean to increase the visibility of the results. This assumption will change only the absolute values, but not the relative difference between two applied IR data sets. The EEP event leads to substantial HO_x (not shown) and NO_x increases. In both cases, NO_x volume mixing ratio is enhanced by more than 10 ppbv above 70 km. The application of the ionization obtained from the balloon measurements results in NO_x abundance exceeding the values obtained with CMIP6 IR in the entire model domain and by more than 100% above 70 km. The ozone depletion is caused mostly by HO_x production and reaches 35% around 75 km. As for NO_x, the application of CMIP6 forcing is less significant for the ozone and overestimates resulting ozone mixing ratio by up to 25%. Below 50 km, the magnitude of chemical responses modeled with IR from balloons is more than 1,000% larger than in case of CMIP6 data (not shown). However, very small absolute values of the chemical response to EEP make the resulting abundances of the chemical species virtually the same. It means that for our particular case, high energy electrons are not important driver of the stratospheric chemistry. It could be different for some other events with higher fluency and harder energy spectrum. Similar conclusions about the role of the bremsstrahlung were made by Xu et al. (2018). It should be noted that the obtained estimates can just indicate how large the uncertainties in CMIP6 forcing set can be but cannot provide full information due to not adequate representation of the downward transport in 1-D models leading to weaker ozone response below 60 km.

4. Conclusion

We discuss interdaily variability of atmospheric ionization during EEP events. We calculate ionization due to EEP in the polar atmosphere retrieved from the long-term balloon observations (Makhmutov et al., 2016) and compare our results with the IR recommended for CMIP6 participants (Matthes et al., 2017) for the same days as the EEP observation from balloons. Above the 0.01-hPa level, IR from both data sets appear to be outside the valid range, as the auroral electrons are not included in CMIP6 data. Balloons (Makhmutov et al., 2016) do not lift higher than 35 km and therefore are hardly sensitive to the auroral electrons which are absorbed at much higher altitudes. Below 1 hPa (altitude less than ~50 km), the IR from balloon observations have much higher values due to secondary bremsstrahlung produced by precipitating electrons have been neglected in CMIP6 data. IR below 50 km caused by the bremsstrahlung have been demonstrated with models of different complexity (e.g., Artamonov et al., 2016b; Rees, 1964). The atmospheric response to this was suggested in several publications (e.g., Frahm et al., 1997, 2000; Xu et al., 2018). Our calculations confirm that the chemical composition response to the bremsstrahlung is small.

Comparison of the atmospheric response to IR from CMIP6 data set and balloon data demonstrates possible uncertainties in the CMIP6 forcing. The simulations with 1-D model shows that the uncertainties in NO_x enhancement can exceed 100%. The ozone depletion simulated with CMIP6 IR is by up to 25% smaller compared to calculations with IR retrieved from balloon observations. These discrepancies in the atmospheric response using different IR data sets are obtained in the altitude band where IR do not differ substantially.

Precipitating electron fluxes are subject of high variability as observed by many experiments (Clilverd et al., 2017; Cresswell-Moorcock et al., 2013; Mironova et al., 2015; Nesse Tyssøy et al., 2016; Woodger et al., 2015). Here we show the difference between IR from the CMIP6 data set and retrieved from balloon measurements (Makhmutov et al., 2016). Our statistical study of about 500 EEP IR profiles during 1961–2006 years shows that variability of EEP detected by balloon measurements exceeds EEP variability of the CMIP6 data set. This difference is not surprising because CMIP6 uses daily values of geomagnetic indices (A_p and *Dst*) as proxies for calculating precipitating electron fluxes and energy spectra. Such an approach, although justified statistically, is far from reality. However, the present knowledge about temporal and spatial variations of EEP is not complete enough to be quantified and incorporated into chemistry-climate models. Nowadays, unprecedented efforts are aimed at the exploration of radiation belts and EEP, including dedicated space mission Van Allen probes (Spence et al., 2013), and the combining ground-based and balloon observations (Clilverd et al., 2017). The forthcoming observational results will form a reliable base for a new parameterization of EEP suitable for the climate community. Our paper will give inspiration for the continuation of the balloon measurements of EEP-related processes using improved instrumentation.

Acknowledgments

The CMIP6 solar forcing data have been taken from http://solarisheppa.geomar.de/cmip6. The spectrum parameters of precipitating electrons have been taken from Makhmutov et al. (2016) and at http://sites.lebedev.ru/ru/DNS_FIAN/479.html. I. M. acknowledges the support of St. Petesburg State University through the grant IAS_11.42.675.2017 (Id: 36360942) and COLLAB2018 (Id: 34828424). A. K. acknowledges the support of St. Petesburg State University through the grant TRAIN2018 (Id: 28176577). G. B. is partly supported by the RFBR grant 16-02-00100. E. R. proposed the idea, compared IR data sets, calculated the atmospheric response, and wrote part of the paper using financial support from the Russian Science Foundation (grant 17-17-01060).

A. A., G. K., I. M., and A. M. thank for support from the Academy of Finland (HEAIM project 314982 and 316223). A. M. was supported by the Academy of Finland (project 272157, Center of Excellence ReSoLVE). This work was done in the frame of the ISSI and the ISSI-BJ project "Relativistic electron precipitation and its atmospheric effect." The work was benefited from the discussion during COST-15211 meetings. The authors thank Dr W. Ball for correcting grammar errors and English usage.

References

Andersson, M. E., Verronen, P. T., Rodger, C. J., Clilverd, M. A., & Seppälä, A. (2014). Missing driver in the Sun-Earth connection from energetic electron precipitation impacts mesospheric ozone. *Nature Communications*, *5*, 5197. https://doi.org/10.1038/ncomms6197

Arsenovic, P., Rozanov, E., Stenke, A., Funke, B., Wissing, J., Mursula, K., et al. (2016). The influence of middle range energy electrons on atmospheric chemistry and regional climate. *Journal of Atmospheric and Solar-Terrestrial Physics*, *149*, 180–190. https://doi.org/10.1016/j.jastp.2016.04.008

Artamonov, A., Mironova, I., Kovaltsov, G., Mishev, A., Plotnikov, E., & Konstantinova, N. (2017). Calculation of atmospheric ionization induced by relativistic electrons with non-vertical precipitation: Update of model CRAC:EPII. *Advances in Space Research*, *59*(9), 2295–2300. https://doi.org/10.1016/j.asr.2017.02.019

Artamonov, A. A., Mishev, A. L., & Usoskin, I. G. (2016a). Model CRAC:EPII for atmospheric ionization due to precipitating electrons: Yield function and applications. *Journal of Geophysical Research: Space Physics*, *121*, 1736–1743. https://doi.org/10.1002/2015JA022276

Artamonov, A. A., Mishev, A. L., & Usoskin, I. G. (2016b). Atmospheric ionization induced by precipitating electrons: Comparison of CRAC:EPII model with a parametrization model. *Journal of Atmospheric and Solar-Terrestrial Physics*, *149*, 161–166. https://doi.org/10.1016/j.jastp.2016.04.020

Calisto, M., Usoskin, I., Rozanov, E., & Peter, T. (2011). Influence of galactic cosmic rays on atmospheric composition and dynamics. *Atmos. Chemical Physics*, *11*(9), 4547–4556. https://doi.org/10.5194/acp-11-4547-2011

Clilverd, M. A., Rodger, C. J., McCarthy, M., Millan, R., Blum, L. W., Cobbett, N., et al. (2017). Investigating energetic electron precipitation through combining ground-based and balloon observations. *Journal of Geophysical Research: Space Physics*, *122*, 534–546. https://doi.org/10.1002/2016JA022812

Comess, M. D., Smith, D. M., Selesnick, R. S., Millan, R. M., & Sample, J. G. (2013). Duskside relativistic electron precipitation as measured by SAMPEX: A statistical survey. *Journal of Geophysical Research: Space Physics*, *118*, 5050–5058. https://doi.org/10.1002/jgra.50481

Cresswell-Moorcock, K., Rodger, C. J., Kero, A., Collier, A. B., Clilverd, M. A., Häggström, I., & Pitkänen, T. (2013). A reexamination of latitudinal limits of substorm-produced energetic electron precipitation. *Journal of Geophysical Research: Space Physics*, *118*, 6694–6705. https://doi.org/10.1002/jgra.50598

Eyring, V., Bony, S., Meehl, G. A., Senior, C. A., Stevens, B., Stouffer, R. J., & Taylor, K. E. (2016). Overview of the Coupled Model Intercomparison Project Phase 6 (CMIP6) experimental design and organization. *Geos Model Development*, *9*, 1937–1958. https://doi.org/10.5194/gmd-9-1937-2016

Fang, X., Randall, C. E., Lummerzheim, D., Wang, W., Lu, G., Solomon, S. C., & Frahm, R. A. (2010). Parameterization of monoenergetic electron impact ionization. *Geophysical Research Letters*, *37*, L22106. https://doi.org/10.1029/2010GL045406

Frahm, R. A., Winningham, J. D., Sharber, J. R., Link, R., Crowley, G., Gaines, E. E., et al. (1997). The diffuse aurora: A significant source of ionization in the middle atmosphere. *Journal of Geophysical Research*, *102*, 28. https://doi.org/10.1029/97JD02430

Frahm, R. A., Winningham, J. D., Sharber, J. R., Link, R., Crowley, G., Gaines, E. E., et al. (2000). Reply to "Comment on 'The diffuse aurora: A significant source of ionization in the middle atmosphere' by R. A. Frahm et al." *Journal of Geophysical Research*, *105*, 15. https://doi.org/10.1029/2000JD900116

Funke, B., Baumgaertner, A., Calisto, M., Egorova, T., Jackman, C. H., Kieser, J., et al. (2011). Composition changes after the "Halloween" solar proton event: The High Energy Particle Precipitation in the Atmosphere (HEPPA) model versus MIPAS data intercomparison study. *Atmospheric Chemistry and Physics*, *11*, 9089–9139. https://doi.org/10.5194/acp-11-9089-2011

Jackman, C. H., Marsh, D. R., Vitt, F. M., Garcia, R. R., Fleming, E. L., Labow, G. J., et al. (2008). Short- and medium-term atmospheric constituent effects of very large solar proton events. *Atmospheric Chemistry and Physics*, *8*, 765–785.

Makhmutov, V. S., Bazilevskaya, G. A., & Krainev, M. B. (2003). Characteristics of energetic electron precipitation into the Earth's polar atmosphere and geomagnetic conditions. *Advances in Space Research*, *31*, 1087–1092. https://doi.org/10.1016/S0273-1177(02)00814-1

Makhmutov, V., Bazilevskaya, G., Stozhkov, Y., Svirzhevskaya, A., & Svirzhevsky, N. (2016). Catalogue of electron precipitation events as observed in the long-duration cosmic ray balloon experiment. *Journal of Atmospheric and Solar-Terrestrial Physics*, *149*, 258–276. https://doi.org/10.1016/j.jastp.2015.12.006

Matthes, K., Funke, B., Andersson, M. E., Barnard, L., Beer, J., Charbonneau, P., et al. (2017). Solar forcing for CMIP6 (v3.2). *Geos Model Development*, *10*, 2247–2302. https://doi.org/10.5194/gmd-10-2247-2017

Meraner, K., & Schmidt, H. (2017). Climate impact of polar mesospheric and stratospheric ozone losses due to energetic particle precipitation. *Atmospheric Chemistry and Physics Diss*, *2017*, 1–14. https://doi.org/10.5194/acp-2017-507

Millan, R. M., McCarthy, M. P., Sample, J. G., Smith, D. M., Thompson, L. D., McGaw, D. G., et al. (2013). The Balloon Array for RBSP Relativistic Electron Losses (BARREL). *Space Science Reviews*, *179*, 503–530. https://doi.org/10.1007/s11214-013-9971-z

Millan, R. M., & Thorne, R. M. (2007). Review of radiation belt relativistic electron losses. *Journal of Atmospheric and Solar-Terrestrial Physics*, *69*, 362–377. https://doi.org/10.1016/j.jastp.2006.06.019

Mironova, I. A., Aplin, K. L., Arnold, F., Bazilevskaya, G. A., Harrison, R. G., Krivolutsky, A. A., et al. (2015). Energetic particle influence on the Earth's atmosphere. *Space Science Reviews*, *194*, 1–96. https://doi.org/10.1007/s11214-015-0185-4

Nesse Tyssøy, H., Sandanger, M. I., Ødegaard, L.-K. G., Stadsnes, J., Aasnes, A., & Zawedde, A. E. (2016). Energetic electron precipitation into the middle atmosphere—Constructing the loss cone fluxes from MEPED POES. *Journal of Geophysical Research: Space Physics*, *121*, 5693–5707. https://doi.org/10.1002/2016JA022752

Picone, J. M., Hedin, A. E., Drob, D. P., & Aikin, A. C. (2002). NRLMSISE-00 empirical model of the atmosphere: Statistical comparisons and scientific issues. *Journal of Geophysical Research*, *107*, 1468. https://doi.org/10.1029/2002JA009430

Rees, M. H. (1964). Ionization in the Earth's atmosphere by aurorally associated Bremsstrahlung X-rays. *Planetary and Space Science*, *12*, 1093–1108. https://doi.org/10.1016/0032-0633(64)90084-4

Rozanov, E., Calisto, M., Egorova, T., Peter, T., & Schmutz, W. (2012). Influence of the precipitating energetic particles on atmospheric chemistry and climate. *Surveys in Geophysics*, *33*, 483–501. https://doi.org/10.1007/s10712-012-9192-0

Seppälä, A., Clilverd, M. A., Beharrell, M. J., Rodger, C. J., Verronen, P. T., Andersson, M. E., & Newnham, D. A. (2015). Substorm-induced energetic electron precipitation: Impact on atmospheric chemistry. *Geophysical Research Letters*, *42*, 8172–8176. https://doi.org/10.1002/2015GL065523

Shapiro, A., Rozanov, E., Egorova, T., Shapiro, A., Peter, T., & Schmutz, W. (2011). Sensitivity of the Earth's middle atmosphere to short-term solar variability and its dependence on the choice of solar irradiance data set. *Journal of Atmospheric and Solar-Terrestrial Physics*, *73*(2), 348–355. https://doi.org/10.1016/j.jastp.2010.02.011

Shprits, Y. Y., Drozdov, A. Y., Spasojevic, M., Kellerman, A. C., Usanova, M. E., Engebretson, M. J., et al. (2016). Wave-induced loss of ultra-relativistic electrons in the Van Allen radiation belts. *Nature Communications*, *7*, 12883. https://doi.org/10.1038/ncomms12883

Smith-Johnsen, C., Marsh, D. R., Orsolini, Y., Nesse Tyssøy, H., Hendrickx, K., Sandanger, M. I., et al. (2018). Nitric oxide response to the April 2010 electron precipitation event: Using WACCM and WACCM-D with and without medium-energy electrons. *Journal of Geophysical Research: Space Physics*, *123*, 5232–5245. https://doi.org/10.1029/2018JA025418

Spence, H. E., Reeves, G. D., Baker, D. N., Blake, J. B., Bolton, M., Bourdarie, S., et al. (2013). Science goals and overview of the Radiation Belt Storm Probes (RBSP) Energetic Particle, Composition, and Thermal Plasma (ECT) Suite on NASA's Van Allen Probes Mission. *Space Science Reviews*, *179*, 311–336. https://doi.org/10.1007/s11214-013-0007-5

Stozhkov, Y. I., Svirzhevsky, N. S., Bazilevskaya, G. A., Kvashnin, A. N., Makhmutov, V. S., & Svirzhevskaya, A. K. (2009). Long-term (50 years) measurements of cosmic ray fluxes in the atmosphere. *Advances in Space Research*, *44*, 1124–1137. https://doi.org/10.1016/j.asr.2008.10.038

Turunen, E., Kero, A., Verronen, P. T., Miyoshi, Y., Oyama, S.-I., & Saito, S. (2016). Mesospheric ozone destruction by high-energy electron precipitation associated with pulsating aurora. *Journal of Geophysical Research: Atmospheres*, *121*, 11852–11861. https://doi.org/10.1002/2016JD025015

van de Kamp, M., Rodger, C. J., Seppälä, A., Clilverd, M. A., & Verronen, P. T. (2018). An updated model providing long-term datasets of energetic electron precipitation, including zonal dependence. *Journal of Geophysical Research: Atmospheres*, *123*, 9891–9915. https://doi.org/10.1029/2017JD028253

van de Kamp, M., Seppälä, A., Clilverd, M. A., Rodger, C. J., Verronen, P. T., & Whittaker, I. C (2016). A model providing long-term data sets of energetic electron precipitation during geomagnetic storms. *Journal of Geophysical Research: Atmospheres*, *121*, 12,520–12,540. https://doi.org/10.1002/2015JD024212

Woodger, L. A., Halford, A. J., Millan, R. M., McCarthy, M. P., Smith, D. M., Bowers, G. S., et al. (2015). A summary of the BARREL campaigns: Technique for studying electron precipitation. *Journal of Geophysical Research: Space Physical*, *120*, 4922–4935. https://doi.org/10.1002/2014JA020874

Xu, W., Marshall, R. A., Fang, X., Turunen, E., & Kero, A. (2018). On the effects of bremsstrahlung radiation during energetic electron precipitation. *Geophysical Research Letters*, *45*, 1167–1176. https://doi.org/10.1002/2017GL076510